ISSN 0027-1314, Moscow University Chemistry Bulletin, 2007, Vol. 62, No. 6, pp. 343–349. © Allerton Press, Inc., 2007.
Original Russian Text © A.I. Stadnichenko, S.V. Koshcheev, A.I. Boronin, 2007, published in Vestnik Moskovskogo Universiteta. Khimiya, 2007, No. 6, pp. 418–426.

Oxidation of the Polycrystalline Gold Foil Surface and XPS Study of Oxygen States in Oxide Layers

A. I. Stadnichenko, S. V. Koshcheev, and A. I. Boronin

Boreskov Institute of Catalysis, Siberian Branch, Russian Academy of Sciences, pr. Akademika Lavrent'eva 5, Novosibirsk, 630090 Russia

e-mail: boronin@catalysis.nsk.su

Received February 20, 2007

Abstract—Gold oxide films obtained on the surface of polycrystalline gold foil upon oxidation by oxygen activated by a high-frequency discharge have been studied by X-ray photoelectron spectroscopy. High-frequency O_2 activation affords oxide films more than 3–5 nm thick. As follows from Au4*f* spectra, the surface gold atoms are oxidized to the oxidation state +3. The O1*s* spectra have a composite shape and are decomposed into four components that characterize nonequivalent states of oxygen in the resulting oxide films. It is assumed that the two major oxygen states (E_b(O1*s*) = 529.0 and 530.0 eV) correspond to the oxygen atoms in two- and three-dimensional gold oxide Au_2O_3, respectively. The oxygen states characterized by the higher binding energies (E_b(O1*s*) = 531.8 and 535.2 eV) likely correspond to molecular oxygen in peroxide and superoxide groups, respectively.

DOI: 10.3103/S0027131407060090

INTRODUCTION

Group IB metals (Cu, Ag) are widely used as active components of catalysts of numerous partial and complete oxidation reactions [1, 2]. It has long been believed that gold does not have such activity [3]. However, in the past 10–15 years since the discovery of the high catalytic activity of nanodispersed gold [1, 4], preparation of nanogold catalysts and study of their physical and chemical properties have attracted much interest [5].

The catalytic activity of gold nanoparticles supported by oxides (TiO_2, Fe_2O_3, CeO_2, etc.) in some reactions (mainly, oxidative) has been found experimentally. Noteworthy are the reactions of low-temperature selective CO oxidation, propylene epoxidation, nitrogen oxide reduction, and SO_2 dissociation. All these reactions involve the formation of adsorbed oxygen species on the surface of gold nanoparticles. It can be assumed that the unique behavior of supported gold catalysts is mainly associated with unusual states of oxygen on the surface of gold nanoparticles. It is not improbable that gold nanoparticles are completely oxidized during oxidation reactions to form nanooxides [6].

In this context, experimental and theoretical study of the structure and the nature of the bond between oxygen and the gold surface is important. First of all, it is of interest to study the direct interaction of oxygen with gold nanoparticles by state-of-the-art spectral methods of surface analysis, such as X-ray photoelectron spectroscopy (XPS), UV photoelectron spectroscopy, Auger electron spectroscopy, and others. It is virtually impracticable to carry out such experiments and to obtain information on the state of adsorbed oxygen on the surface of gold nanoparticles because of the low concentration of these particles and the overlap of strong oxygen lines arising from the oxide supports. An alternative way is to study adsorbed oxygen on a bulk gold surface (foil, single crystals, powders). It is evident that no one can insist on the identity of the properties of bulk and nanosized gold. Nevertheless, data on oxygen species obtained for bulk gold can serve as a basis for correct interpretation of the spectra and properties of nanoparticles. However, study of bulk gold samples encounters a substantial obstacle, namely, the difficulty of obtaining oxygen species on the gold surface because of the high barrier to O_2 adsorption [7, 8]. Different methods have been suggested for treating the gold surface and obtaining chemisorbed oxygen on it: action of ozone [9], NO_2 [10], and atomic oxygen [11, 12]; oxygen adsorption at high pressures and temperatures [13]; and others. These methods are either of low efficiency or rather inconvenient. For efficient oxidation of the gold surface, electrochemical oxidation of a gold electrode [14] or treatment with oxygen activated by a high-frequency discharge [15, 16] has been suggested. When electrochemical oxidation is used, it is difficult to combine the XPS method with an electrochemical cell; at the same time, high-frequency activation can easily be carried out in the chambers of an electronic spectrometer.

As distinct from the electrochemical method, exposure to oxygen plasma is implied to produce only one type of gold oxide, Au_2O_3 [17, 18]. However, as is known, the silver (gold analogue in Group IB) surface is intensively oxidized by a microwave oxygen dis-

charge to produce not only a thick oxide film but also several oxygen species and states with considerably different chemical properties [19, 20]. Two major types of oxide structures are formed, one of which is cuprite-type Ag_2O. In the second state, oxygen is believed to be involved in AgO particles [20] or in oxidized nanoparticles with the molecular nature of oxygen bonding AgO_n with $n > 1$ [19]. In any case, low-temperature plasma treatment of the silver surface imparts new properties to the oxygen in oxide structures. It is possible that specificity in the formation of oxide species obtained on the gold surface under oxygen activation also persists on the surface of gold nanoparticles where O_2 is adsorbed without activation.

This work deals with the study of oxide layers formed on the gold foil surface at room temperature upon plasma treatment.

EXPERIMENTAL

Measurements were carried out on a VG ESCALAB HP photoelectron spectrometer. The instrument consisted of two high-vacuum chambers for pretreatment of samples and an analyzer chamber, which are separated by shut-off valves. The spectrometer was equipped with an X-ray source with a double Mg/Al anode, which made it possible to use for excitation primary MgK_α (1253.6 eV) and AlK_α (1486.6 eV) radiation. A hemispherical electrostatic analyzer was used for analysis of the photoelectron energy spectrum. X-ray photoelectron spectra were recorded in the constant pass energy (HV) mode. General spectra were recorded at HV = 100 eV, and detailed Au4*f*, O1*s*, and C1*s* spectra were recorded at HV = 20 eV (energy step, 0.1 eV). In this case, the line width at half maximum for the reference Au4$f_{7/2}$ line was 1. 3 eV. The Au4$f_{7/2}$ binding energy (84.0 eV) was used as the internal reference. Processing of the data obtained and analysis of the spectra were performed with the PSILON and CALC programs tested for a number of systems [21–23] and with standard graphical software.

In the pretreatment chamber, an ion gun for sample purification and an antenna for high-frequency discharge generation were mounted. The sample was a polycrystalline gold (99.99% purity) sheet 0.2 mm thick. A piece of the plate, 10×10 mm, was fastened by gold wires with tantalum springs at the ends. The tantalum springs ensured the stable position of the sample relative to the X-ray beam and the analyzer lens during recording of spectra at different temperatures.

Before the experiments, the sample was repeatedly purified by etching its surface with argon ions followed by annealing at 873 K. After these operations, XPS showed no impurities.

The antenna for high-frequency discharge was a gold (99.99%) wire 0.2 mm in diameter. The choice of the antenna material was not accidental since HF discharge generation can be accompanied by sputtering of atoms from the antenna material. If the antenna material is the same as that of the sample, such a construction makes it possible to minimize sputtering of impurities from other parts of the oxygen excitation system (in the course of experiments, no impurity deposition on the sample surface was observed). The process was monitored by XPS. High-frequency oxygen activation was carried out at an adjustable frequency of about 12.6 MHz at oxygen pressures of 1–100 Pa. The exposure to activated oxygen was 1–10 min. During exposure to activated oxygen, the sample temperature was varied from 300 to 520 K and a potential with discrete values in the range from +300 to –300 V was applied to the sample.

RESULTS AND DISCUSSION

State of Gold Atoms upon High-Frequency Oxidation of Polycrystalline Gold Foil

Oxygen activated by a high-frequency discharge efficiently interacts with the polycrystalline gold foil surface. Figure 1 shows that the action of oxygen plasma leads to a sharp decrease in the intensity of the metal gold doublet in the Au4*f* spectra (E_b = 84.0 and 87.0 eV) and to the emergence of a strong doublet with E_b = 85.6 and 89.2 eV. According to the published data, this doublet is due to gold incorporated in Au_2O_3 [11, 12, 14–17]. This is evidence of the growth of a three-dimensional oxide film. The decomposition of the Au4*f* spectra into components shows that only two gold states—metallic and oxidized (Fig. 2)—are observed after the action of high-frequency discharge.

The thickness of the resulting oxide film can be varied by changing the surface treatment duration. Figure 1 shows that, at the early stage of exposure of the gold foil surface to activated oxygen, the oxide film grows rather rapidly (this can be judged from the buildup of the oxide component in the Au4*f* spectrum with E_b(Au4*f*) = 85.6 eV), whereas an increase in the treatment duration to 1 min or more leads to a noticeable decrease in the film growth rate. In particular, after a 10-min exposure to oxygen activated by a high-frequency discharge, the X-ray photoelectron spectra show a weak doublet due to metallic gold. This can be evidence that the thickness of the oxide film is ~90 Å. It is likely that the oxide film growth occurs by means of diffusion of gold atoms through the oxide film to the surface. The action of X-ray radiation on ionic compounds of Group IB metals is also possible; i.e., the gold oxide on the surface decomposes during recording of the photoelectron spectrum. The effect of X-ray radiation on the reduction of divalent copper is well known [22]. It is likely that a thin metal film will always cover the gold oxide surface when the gold oxide states are studied by probe spectral methods. On the whole, the question of whether gold oxide particles are reduced during XPS measurements requires a separate consideration.

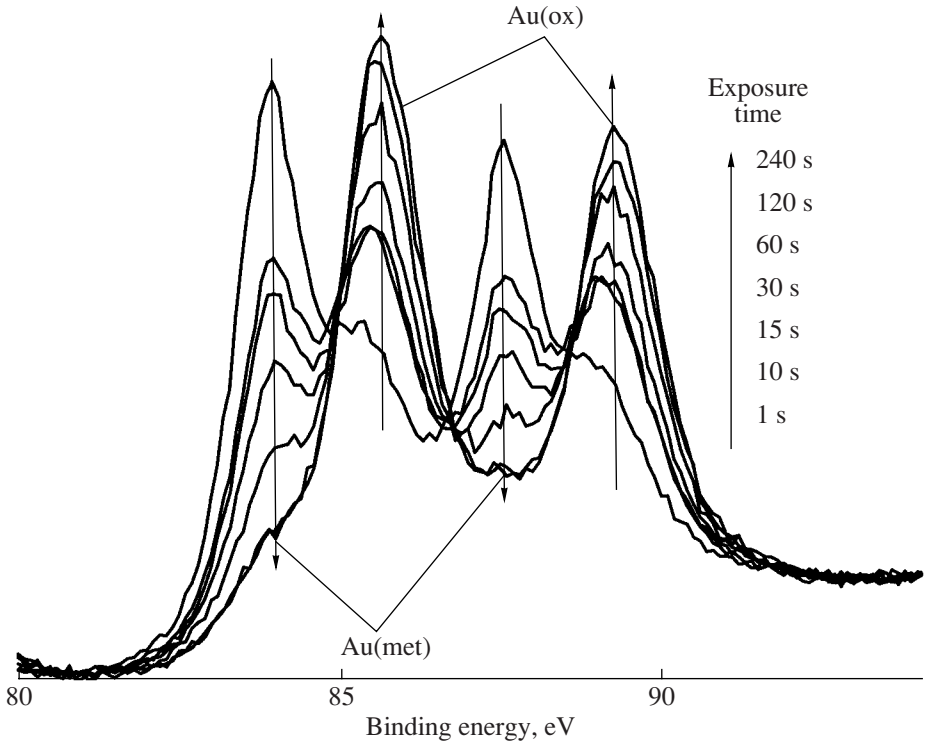

Fig. 1. Au4*f* spectra recorded after exposure of the polycrystalline gold foil surface to oxygen activated by microwave discharge in the gas phase as a function of exposure time. Treatment conditions: $P(O_2)$ = 25 Pa; T = 300 K; U = +300 V; and the treatment duration (τ) was 1, 10, 15, 30, 60, 120, and 240 s.

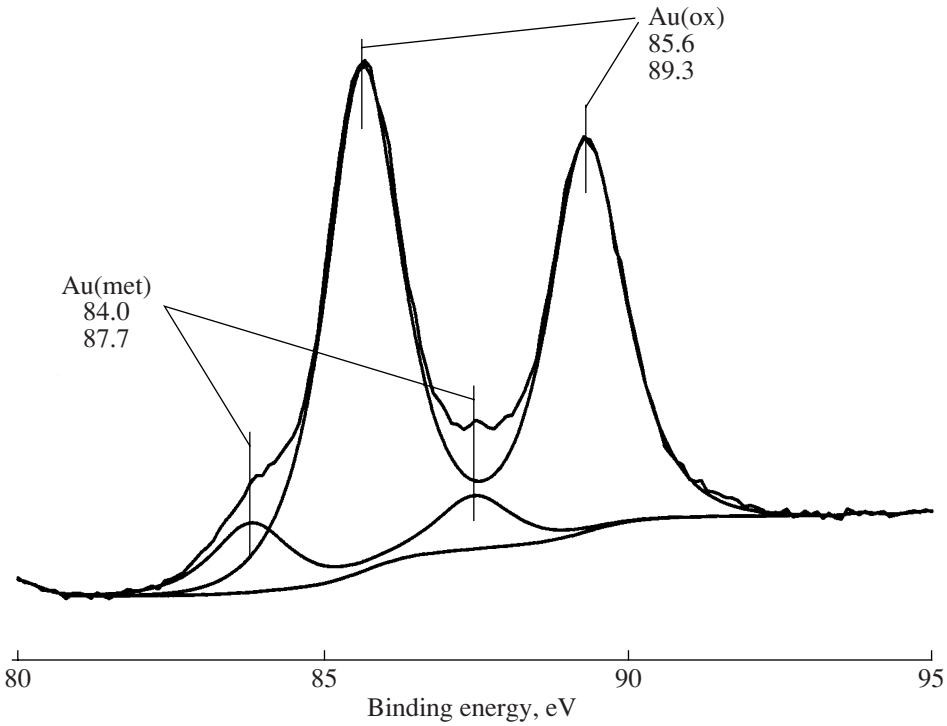

Fig. 2. Spectral decomposition of the Au4*f* spectrum recorded after exposure of the polycrystalline gold foil surface to oxygen activated by microwave discharge in the gas phase. Treatment conditions: $P(O_2)$ = 25 Pa, T = 300 K, U = +300 V, and τ = 240 s.

It should be noted that the formation of rather thick silver oxide films (>30 Å) has been observed upon oxidation of the silver surface by oxygen activated by a high-frequency discharge [19, 20]; however, the Au4*f* spectra reported in [15] show that, upon gold oxidation, the oxide component does not exceed the metallic one. This means that the gold oxide film is about 15–20 Å thick. In our case, the metallic component constitutes no more than 5–10%, which points to a higher degree of oxidation of the polycrystalline gold foil surface; i.e., the film thickness in our experiments is considerably larger and constitutes 30–40 Å or more. It is not inconceivable that this high efficiency of interaction of activated oxygen with the gold foil surface is associated not only with the parameters of the HF discharge but also with the fact of using a gold wire as the antenna. The routine material used for manufacturing antennas is superpure aluminum, which has the lowest sputtering yield in an oxygen atmosphere. It is possible that, in the course of experiments, the gold from the antenna was sputtered under the action of the high-frequency discharge and the oxide film growth was due to both the interaction of activated oxygen with the gold foil surface and gold sputtering in an oxygen atmosphere. Such a method of obtaining gold oxides was described previously [23]. However, in this case, the oxide film growth rate should not depend strongly on the oxide film thickness (which was not observed in the experiments).

The use of an aluminum antenna in high-frequency discharge shows that the O1*s* and Au4*f* spectra characterize the same states of gold and oxygen atoms as were obtained with the use of the gold antenna. In addition, no aluminum was detected on the sample surface within the sensitivity of XPS. Thus, we can assume that no noticeable sputtering of the gold antenna material occurs and that the film growth is mainly driven by interaction of activated oxygen with the polycrystalline gold foil surface.

A change in the potential applied to a sample has no significant effect on the oxide film growth or on stabilization of some specific oxygen species as in the case of oxygen adsorption on the silver foil surface [19]. However, it is worth noting that, at long high-frequency discharge times, the activated oxygen interacts with chamber walls to yield metal oxides, in particular, iron oxides highly mobile in an oxygen atmosphere, on the sample holder. We found that a positive potential applied to the sample during treatment with oxygen under high-frequency excitation leads to a decrease in the amount of iron oxides on the gold surface. We also found that, at exposure times above 5 s, a change in the oxygen pressure within the range 5–100 Pa and in the distance between the sample and antenna has no effect on the thickness and quality of the formed oxide film. It is likely due to the fact that the basic parameters of high-frequency oxygen activation (excitation frequency, O_2 pressure, etc.) used in this series of runs lead to rather efficient oxygen activation independent of auxiliary parameters.

Oxygen State upon High-Frequency Oxidation of the Polycrystalline Gold Foil Surface

The interaction of the gold surface with oxygen in high-frequency discharge leads to the emergence of a strong O1*s* line with E_b(O1*s*) = 530.0 eV and a weaker line with $E_b \approx 535.5$ eV (Fig. 3). However, at short exposure times, the major oxygen line with E_b(O1*s*) ≈ 530.0 eV is shifted toward smaller binding energies by about 0.3 eV and the line with $E_b \approx 535.5$ eV vanishes. For the major O1*s* line, the width at half maximum exceeds 2 eV, the line being noticeably asymmetric. This can mean that this oxygen line is composite and, most likely, consists of several components; i.e., there are several nonequivalent states of oxygen atoms in the resulting gold oxide films.

The spectra were decomposed into components of Gaussian–Lorentzian shape with a spectrum-decomposition program. The error of determination of binding energies was no more than 0.1 eV. The assumption of a Gaussian–Lorentzian shape of the O1*s* line is well justified since oxygen atoms have no *d* or *f* electrons and have only *s* and *p* electrons. Figure 4 shows the decomposition of the O1*s* spectrum after the treatment of gold foil with high-frequency discharge for 4 min. The integral O1*s* peak is decomposed into four components: peak α_1 with E_b = 529.0 eV, peak α_2 with E_b = 530.0 eV, peak α_3 with E_b = 532.1 eV, and peak α_4 with E_b = 535.2 eV. For convenience of discussion, the same designations α_1–α_4 are used below. As follows from the decomposition in Fig. 4, the oxygen in the oxide films is mainly in two states, α_1 and α_2, the buildup of the O1*s* peak with an increase in the plasma exposure time being mainly due to an increase in the contribution of component α_2. This is responsible for the shift of the O1*s* peak toward larger binding energies with an increase in the time of exposure of the gold foil surface to activated oxygen. Consideration of the spectral features of the O1*s* spectra together with those of the Au4*f* spectra shows that the oxide component with E_b = 85.6 eV is related to oxygen of both α_1 and α_2 states incorporated in the three-dimensional gold oxide phase Au_2O_3.

Component α_1 with E_b = 529.0 eV is observed in X-ray photoelectron spectra after exposures to oxygen plasma of different durations, beginning with the shortest times. It is worth noting that an increase in the exposure time does not lead to a buildup of the α_1 and α_2 components. The lower E_b value for the oxygen in the α_1 state as compared with that for the oxygen in the α_2 state allows us to assume that the charge state of α_1 species is close to that of atomic oxygen on the surface, since its position coincides with E_b(O1*s*) = 529.4 ± 0.2 eV obtained for atomic oxygen at the gold foil surface [9, 11]. This assumption is quite reasonable since the high-frequency oxygen discharge generates both excited molecular states of oxygen and atomic oxygen. It is not improbable that this α_1 species can be due to two-dimensional gold oxide and the oxygen species

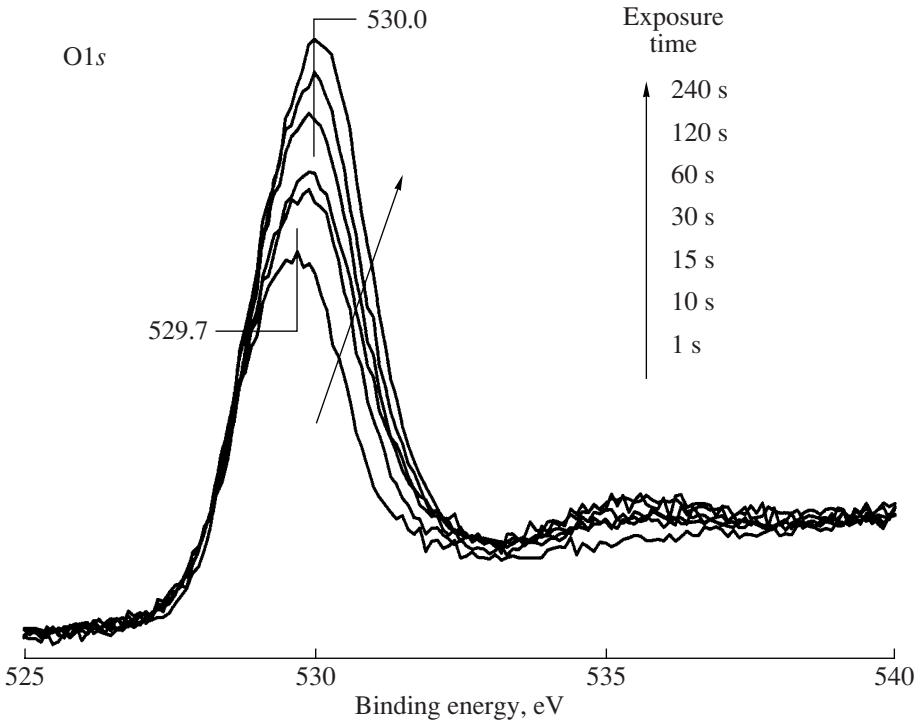

Fig. 3. O1*s* spectra recorded after exposure of the polycrystalline gold foil surface to oxygen activated by microwave discharge in the gas phase as a function of exposure time. Treatment conditions: $P(O_2)$ = 25 Pa; T = 300 K; U = +300 V; and τ was 1, 10, 15, 30, 60, 120, and 240 s.

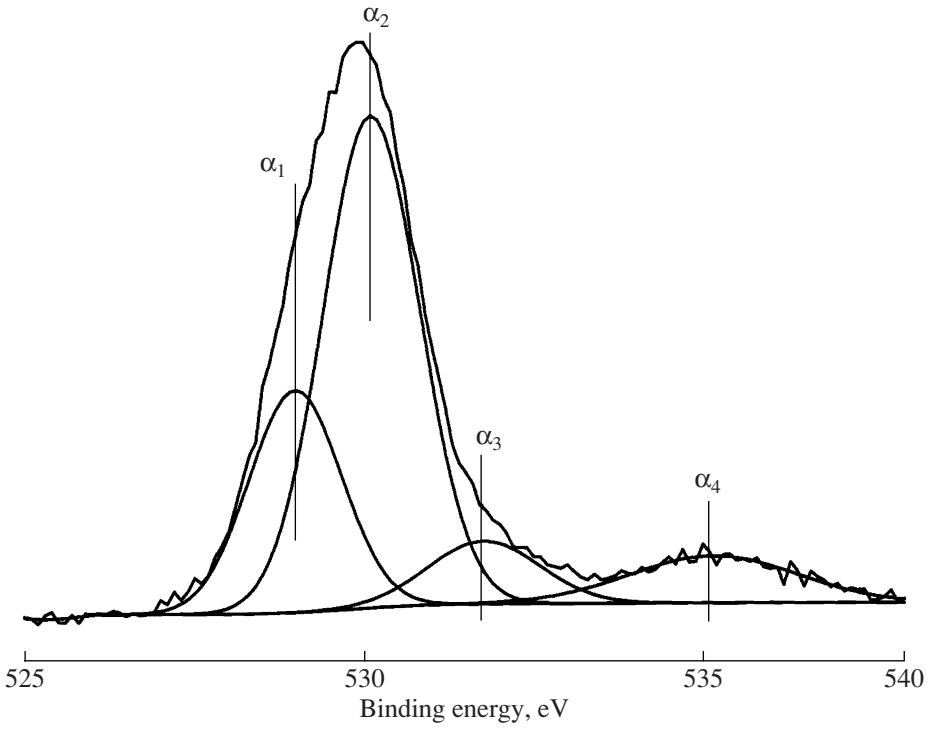

Fig. 4. Spectral decomposition of the O1*s* spectrum recorded after exposure of the polycrystalline gold foil surface to oxygen activated by microwave discharge in the gas phase. Treatment conditions: $P(O_2)$ = 25 Pa, T = 300 K, U = +300 V, and τ = 240 s. The peak positions are 529.0 (α_1), 530.0 (α_2), 531.8 (α_3), and 535.2 eV (α_4).

with E_b(O1*s*) = 530.1 eV is incorporated in three-dimensional gold oxide; however, there is no definite proof of these assumptions. Thus, the gold oxide film is characterized by two major nonequivalent oxygen states, with their proportion changing during surface oxidation: α_1 species forms at the early stages of interaction of activated oxygen with the gold surface and saturates rather rapidly, whereas species α_2 mainly forms upon deeper oxidation.

The binding energy of oxygen species α_3 (E_b(O1*s*) = 531.8 eV) is rather high for atomic oxygen adsorbed at metal surfaces. This species forms upon long-term exposure to activated oxygen. Sometimes, high binding energies are attributed to the molecular state of oxygen [24]; however, it is also assumed that similar binding energies should correspond to the oxygen of OH groups or water molecules on the gold surface [14, 15, 25]. This possibility cannot be completely ruled out; however, the persistence of this oxygen species and its constant amount allow us to cast doubt on this assumption. It is most likely that this component corresponds to the oxygen incorporated either directly in the oxide film or in the transition layer between the metal substrate and oxide film. The value E_b = 531.8 eV points to the existence of a direct chemical bond between oxygen atoms; i.e., we can assume, in line with [25], the existence of peroxide and superoxide species stable at room temperature. Molecular oxygen is fixed most likely on tiny particles and the amorphized gold surface [6].

Long-term treatment with oxygen activated by a high-frequency discharge leads not only to efficient oxidation of the gold surface but also to the formation of a new unique oxygen state responsible for the peak separated from the basic O1*s* peak by 5.5 eV (α_4). The binding energy of this species (535.5 eV) is anomalously high for a thermostable oxygen form, since only weakly adsorbed or physisorbed oxygen species have been described as having such high binding energies E_b(O1*s*) [26]. This oxygen species is not generated at early stages of gold oxidation; rather, it is observed only at a high degree of coverage of the surface with oxygen; therefore, we can assume that the appearance of this species is related to the formation of a thick gold oxide film. To explain the chemical nature of this species, two hypotheses can be put forth.

(1) This species is molecular oxygen occluded in interblock or intergrain voids of the oxide film or of the metal–oxide interface layer. Oxygen can be occluded due to an extremely rapid growth of an oxide on the surface under plasma treatment. As a result, oxygen turns out to be entrapped in cavities and voids of the nascent oxide with heterogeneous morphology. This hypothesis is supported by the fact that oxygen in the gas phase has a similar binding energy, E_b(O1*s*) = 537–538 eV (with inclusion of the work function of a spectrometer). Indirect evidence in favor of the hypothesis of occluded gas can be the oxygen peak with a close binding energy (E_b = 535.7 eV) observed after sputtering of gold on the gold foil surface in the presence of oxygen [25]. In any case, this species is close to the superoxide oxygen structure.

(2) Photoionization takes place when elastic loss of electrons due to electron shake-up leads to the emergence of shake-up satellites in spectra. A similar situation is observed for some oxide and carbon systems, in particular, in copper oxide CuO, graphite, and others [24]. It is worth noting that copper is a gold analogue in the group; however, for copper oxide, satellites are observed only in Cu2*p* spectra. It is not improbable that the satellite lines in the range 534–537 eV arise from molecular oxygen in the system (α_3) and the emergence of the shake-up satellite in O1*s* spectra is caused by the electronic structure of the occupied and vacant orbitals of the O–O bond.

Our study of the thermal stability of the resulting oxide films showed that all oxygen species are stable up to about 470 K. At 470 K, the amount of oxygen on the gold surface slightly decreases. However, heating to 480 K is accompanied by vigorous decomposition of gold oxide and oxygen desorption with recovery of the metallic state of the surface.

Our data on the thermostability of gold oxide Au_2O_3 are consistent with the data in [9, 11]. At the same time, a thermostability of gold oxide not exceeding 370 K has been reported [15, 18]. It is likely that oxide films obtained in different works differ in structure and morphology and require further, detailed study by different spectral and structural methods of surface analysis.

CONCLUSIONS

Oxide films formed on the gold foil surface upon high-frequency activation of O_2 have been studied by XPS. Optimization of O_2 activation parameters makes it possible to obtain oxide films more than 3–5 nm thick. High-frequency activation of oxygen in the gas phase allows uncontrolled deposition of impurities on the surface to be avoided. The Au4*f* spectra showed that gold atoms on the oxidized surface are in the oxidation state +3. The O1*s* line shape is complicated and consists of four components characterizing nonequivalent oxygen states in the resulting oxide films. It is assumed that the two major oxygen states correspond to oxygen incorporated in two-and three-dimensional gold oxide Au_2O_3 (E_b(O1*s*) = 529.0 and 530.0 eV, respectively). The oxygen state with E_b(O1*s*) = 531.8 eV corresponds presumably to the oxygen of peroxide groups. The nature of the fourth oxygen state, which gives rise to the high-energy peak with E_b(O1*s*) = 535.5 eV, is not completely clear. The most rational explanation is that this oxygen species corresponds to superoxide-type molecular oxygen occluded in the oxide film.

ACKNOWLEDGMENTS

This work was supported through grant no. 8051 of the subprogram "Development of the Potential of

Higher Education." A.I. Stadnichenko is grateful to the Zamoraev Foundation for a graduate scholarship (2005).

REFERENCES

1. Masatake Haruta, *Appl. Catal. A: General*, 2001, vol. 222, p. 427.
2. Boccuzzi, F., Chiorino, A., Manzoli, M., Andreeva, D., Tabakova, T., Ilieva, L., and Iadakiev, V., *Catal. Today*, 2002, vol. 75, p. 169.
3. Hammer, B. and Norskov, J.K., *Nature*, 1995, vol. 376, p. 238.
4. Haruta, M., Yamada, N., Kobayashi, T., and Iijima, S., *J. Catal.*, 1989, vol. 115, p. 301.
5. Bond, G.C. and Thompson, D.T., *Catal. Rev.–Sci. Eng.,* 1999, vol. 41, nos. 3–4, p. 319.
6. Dong Chan Lim, Ignacio Lopez-Salido, Rainer Dietsche, Moritz Bubek, and Yong Lok Kim, *Surf. Sci.*, 2006, vol. 600, p. 507.
7. Zhi-Pan Liu, Hu, P., and Ali Alavi, *J. Am. Chem. Soc.*, 2002, vol. 124, p. 14770.
8. Wallace, W.T., Wyrwas, R.B., Whetten, R.L., et al., *J. Am. Chem. Soc.*, 2003, vol. 125, p. 8408.
9. Saliba, N., Parker, D.H., and Koe, B.E., *Surf. Sci.*, 1998, vol. 410, p. 270.
10. Wickham, D.T., Banse, B.A., and Koe, B.E., *Catal. Lett.*, 1990, vol. 6, p. 163.
11. Canning, N.D.S., Outka, D., and Madix, R.J., *Surf. Sci.*, 1984, vol. 141, p. 240.
12. Linsmeier, C. and Wanner, J., *Surf. Sci.*, 2000, vol. 305, p. 454.
13. Chevrier, J., Huang, L., Zeppenfeld, P., and Comsa, G., *Surf. Sci.*, 1996, vol. 355, p. 1.
14. Juodkazias, K., Juodkazyte, J., Jasulaitiene, V., Lukinskas, A., and Sebeka, B., *Electrochem. Commun.*, 2000, vol. 2, p. 503.
15. Koslowski, B., Boyen, H.-G., Wilderotter, C., Kastle, G., Ziemann, P., Wahrenburg, R., and Oelhafen, P., *Surf. Sci.*, 2001, vol. 475, p. 1.
16. McClure, S.M., Kim, T.S., Stiehl, J.D., Tanaka, P.L., and Mullins, C.D., *J. Phys. Chem. B*, 2004, vol. 108, p. 17952.
17. Evans, S., Evans, E.L., Parry, D.E., Tricker, M.J., Walters, M.J., and Thomas, J.M., *Faraday Disc. Chem. Soc.*, 1974, vol. 58, p. 97.
18. Tsai, H., Hu, E., Perng, K., Chen, M., Wu, J.-C., and Chang, Y.-S., *Surf. Sci. Lett.*, 2003, vol. 537, p. 447.
19. Boronin, A.I., Koscheev, S.V., Murzakhmetov, K., et al., *Appl. Surf. Sci.*, 2000, vol. 165, p. 9.
20. Bielmann, M., Schwaller, P., Ruffieux, P., Groining, O., Schlapbach, L., and Groining, P., *Phys. Rev. B: Condens. Matter*, 2002, vol. 65, p. 235431.
21. Slavinskaya, E.M., Chesalov, Yu.A., Boronin, A.I., Polukhina, I.A., and Noskov, A.S., *Kinet. Catal.*, 2005, vol. 46, no. 4, p. 555.
22. Titkov, A.I., Salanov, A.N., Koscheev, S.V., and Boronin, A.I., *React. Kinet. Catal., Lett.*, 2005, vol. 86, no. 2, p. 371.
23. Knyazev, A.S., Magaev, O.V., Vodyankina, O.V., Titkov, A.I., Salanov, A.N., Koshcheev, S.V., and Boronin, A.I., *Kinet. Katal.*, 2004, vol. 45, no. 6, p. 8.
24. *Practical Surface Analysis by Auger and X-ray Photoelectron Spectroscopy*, Briggs, D. and Seah, M.P., Eds., Chichester: Wiley, 1983. Translated under the title *Analiz poverkhnosti metodami ozhe- i rentgenovskoi fotoelektronnoi spektroskopii*, Moscow: Mir, 1987.
25. Pireaux, J.J., Liehr, M., Thiry, P.A., Delrue, J.P., and Caudano, R., *Surf. Sci.*, 1984, vol. 141, p. 221.
26. Carley, A.F. and Davies, P.R., Oxygen States at Metal Surfaces, in *Interfacial Science (IUPAC Chemistry for the 21st Century)*, Roberts, M.W., Ed., Oxford: Blackwell, 1997, p. 77.